Japanese Journal of Radiology (2019) 37:660–665
https://doi.org/10.1007/s11604-019-00856-w

TECHNICAL NOTE

The opacity of mineral ion-loaded bead (DC beads®) on low-keV monochromatic images from dual energy CT and T1-weighted gradient-echo MRI

Keizo Tanitame[1] · Nobuko Tanitame[2] · Yuji Takahashi[3] · Erika Tamai[4] · Taichi Kurose[1]

Received: 3 June 2019 / Accepted: 11 July 2019 / Published online: 23 July 2019

Abstract

Purpose To evaluate the opacity of DC beads® (DCB) loaded with mineral ions on low-keV monochromatic images from dual energy computed tomography (DECT) and T1-weighted gradient-echo (T1-GRE) MRI.

Materials and methods Fe^{2+} or Ca^{2+}-loaded DCBs were prepared by mixing DCBs in 100 mM $FeSO_4$ or $CaSO_4$ solution and scanned by DECT from 10 min to 27 h after mixing. The Hounsfield units (HUs) of sedimented DCBs on 40-keV monochromatic images were measured. Next, we mixed DCBs in 100, 10, 5 and 1 mM $FeSO_4$ solutions, and scanned these solutions from 15 to 120 min after mixing using a 3 T MR scanner. The signal–noise ratios (SNRs) of sedimented DCBs on T1-GRE were measured. Venous blood was scanned to compare with DCBs.

Results The CT values of DCBs in $FeSO_4$ and $CaCl_2$ solutions gradually increased, and were 113.3 and 43.1 HU at 27 h, respectively; that of blood was 17.8 HU. The SNR of DCB in 1 mM $FeSO_4$ solution increased and achieved equilibrium at 120 min, and was 120.5 and higher than in the other $FeSO_4$ solutions. The SNR of blood was 49.7.

Conclusion Optimally Fe^{2+}-loaded DCBs can be discriminated from venous blood on 40-keV monochromatic images from DECT and T1-GRE.

Keywords DC beads · Fe^{2+} · Ca^{2+} · Dual energy CT · MRI

Introduction

Transarterial chemoembolization (TACE) or transarterial embolization (TAE) has been performed as a minimally invasive treatment for some benign and unresectable malignant hypervascular tumors or arteriovenous malformations [1]. Recently, drug eluting bead TACE (DEB-TACE) has merged as an advancement of conventional TACE with the potential for the selective delivery of a large amount of anticancer drug to the tumors and less systemic toxicity [2–4]. Although some spherical embolic agents such as DC beads® (DCB; Eisai Co., Tokyo, Japan), Hepasphere® (Nihon Kayaku Co., Tokyo, Japan), and Embosphere® (Nihon Kayaku Co., Tokyo, Japan) are utilized in Japan, they are lucent on X-ray fluorography, computed tomography (CT) and magnetic resonance imaging (MRI), and that makes it difficult to evaluate the embolization effect.

Radiopaque embolic agents make it possible to visualize the distribution of the agents in targeted tumors and to guide subsequent treatments, such as repeated embolization or radiofrequency ablation therapies. DC Bead LUMI® (Biocompatibles UK Ltd., Farnham, UK) [5–7] is the first commercially available radiopaque drug-eluting bead in Europe, and other radiopaque embolic microspheres (X-spheres [8], lipiodol-loaded DCBs [9, 10], TaCaAlg-microsphere [11], Embozene with barium sulfate [12]) are also evaluated in clinical practice or research.

Furthermore, polyvinyl alcohol (PVA) particles loaded with gadolinium-diethylenetriamine penta-acetic acid

✉ Keizo Tanitame
tntrad@gmail.com

1 Department of Diagnostic Radiology, Hiroshima Prefectural Hospital, Minami-ku, Ujinakanda, 1−5−54, Hiroshima 734-8530, Japan

2 Department of Radiology, Hiroshima City Hiroshima Citizens Hospital, Hiroshima, Japan

3 Department of Clinical Radiology, Hiroshima University Hospital, Hiroshima, Japan

4 Department of Radiology, Hiroshima Prefectural Hospital, Hiroshima, Japan

(Gd-DTPA) [13], holmium-loaded microsphere [14] and iron oxide-containing embosphere [15] are reported to be visible on MRI.

DCB is based on a biocompatible polyvinyl alcohol (PVA) hydrogel that is modified with negatively charged sulfonyl groups [16]. The increased number of sulfonyl moieties permits cationic antineoplastic drugs to be loaded. We thought that mineral ions could covalently bind to sulfonyl groups of DCB, and mineral ion-loaded DCBs could be visible on CT and MRI.

The purpose of this study is to evaluate the opacity of DCBs loaded with mineral ions on low-keV monochromatic images from dual energy CT (DECT) scan and T1-weighted gradient-echo (T1-GRE) MRI.

Materials and methods

We mixed DCB of 100–300 μm in diameter in 0.5 ml of distilled water, 100 mmol/l (mM) $FeSO_4$ and 100 mM $CaCl_2$ solutions at the temperature of 25 °C, and scanned the solutions at 10 and 30 min, 1, 3, 6, 9, 18 and 27 h after mixing using a rapid kv-switching single-source DECT scanner (GE Revolution GSI, GE Healthcare, Milwaukee, USA). Pure distilled water, 100 mM $FeSO_4$ and 100 mM $CaCl_2$ solutions not containing DCB were also scanned as controls. The DECT employed two different kV energies for CT image acquisition, and we used following acquisition parameters: rotation time 0.8 s, collimation 64 × 0.625 mm, helical pitch 0.531, field of view (FOV) 160 × 160 mm, peak tube voltage switching from 80 to 140 kV, and tube current 260 mA. The image data were reconstructed into contiguous 0.625-mm-thick slices at 2 virtual monochromatic levels: 40- and 70-keV using an advantage workstation (AW VolumeShare 7 Workstation, GE Healthcare, Chicago, Illinois, USA). The Hounsfield units (HUs) of sedimented DCBs on 40- and 70-keV monochromatic images were measured and their spectral HU curves were compared.

Next, we mixed the DCB in 0.5 ml of distilled water, 100, 10, 5 and 1 mM $FeSO_4$ solutions at the temperature of 25 °C, and scanned these solutions at 15, 30, 60, 90 and 120 min after mixing using a 3 T MR scanner (Philips INGENIA 3.0 T, Best, The Netherlands; gradient strength = 40 mT/m, slew rate = 150 T/m/s) and an 8-channel head coil. Pure distilled water, 100, 10, 5 and 1 mM $FeSO_4$ solutions not containing DCB were also scanned as controls. Axial two-dimensional T1-weighted gradient echo (T1-GRE) was optimized as follows: repetition time (TR) 170 ms, echo time (TE) 2.3 ms, flip angle (FA) 60°, FOV 200 × 200 mm, matrix 256 × 256, slice thickness/gap 2/0.2 mm, number of signals averaged (NSA) 5, scan time 2 m 57 s. The signal–noise ratios (SNRs) of sedimented DCBs on T1-GRE were measured.

Fresh venous blood was also scanned with DECT and MRI scanners to compare with Fe^{2+}- or Ca^{2+}-loaded DCBs. Considering the interobserver differences, two radiologists (K.T. and N.T.) analyzed CT and MR images, independently, and the average values from the two readers were collected as the final result.

In addition, digital macrophotography was used for evaluating aggregation of Fe^{2+}-loaded or Ca^{2+}-loaded DCB particles at 27 h after mixing as compared with unloaded DCBs.

Results

The CT values of DCBs in 100 mM $FeSO_4$ and 100 mM $CaCl_2$ solutions gradually increased in processing time, and achieved plateau values at 27 h after mixing (113.3 and 43.1 HU on a 40-keV monochromatic image and 49.1 and 24.4 HU on a 70-keV monochromatic image, respectively) (Fig. 1). The CT values of DCB in distilled water and fresh venous blood were − 28.7 and 17.8 HU on the 40-keV image, respectively; those were − 1.1 and 31.9 HU on the 70-keV image, respectively. The contrast between Fe^{2+}-loaded DCB in 100 mM $FeSO_4$ solution at 27 h after mixing and fresh venous blood on the 40-keV image was most distinct.

On spectral HU curve calculated from the image data at 27 h after mixing, the CT values of Fe^{2+}-loaded DCB and Ca^{2+}-loaded DCB increased as photon energy decreased, while fresh venous blood showed an increase trend in CT values as photon energy increased (Fig. 2).

The SNR of DCB in 1 mM $FeSO_4$ solution increased and achieved nearly equilibrium at 120 min after mixing, and was 120.5 and higher than those of DCBs in 100, 10 and 5 mM $FeSO_4$ solutions, which were 16.0, 52.0 and 119.2, respectively (Fig. 3). The SNRs of DCB in distilled water and fresh venous blood were 22.6 and 49.7, respectively. Fe^{2+}-loaded DCB in 1 mM $FeSO_4$ solution at 120 min after mixing and fresh venous blood were discriminated most clearly on T1-GRE.

Fe^{2+}-loaded or Ca^{2+}-loaded DCB particles did not aggregate in distilled water on the microphotography. They were seen to maintain their original size and shape after loading, but their color became darker than unloaded DCB particles (Fig. 4).

Discussion

Several spherical embolic agents have been employed for DEB-TACE or TAE during past two decades [1–4], and recently it has been reported that radiopaque [5–12] or MRI-opaque embolic agents [13–15] are useful in clinical practice or research. As Fe^{2+} and Ca^{2+} ions are human plasma

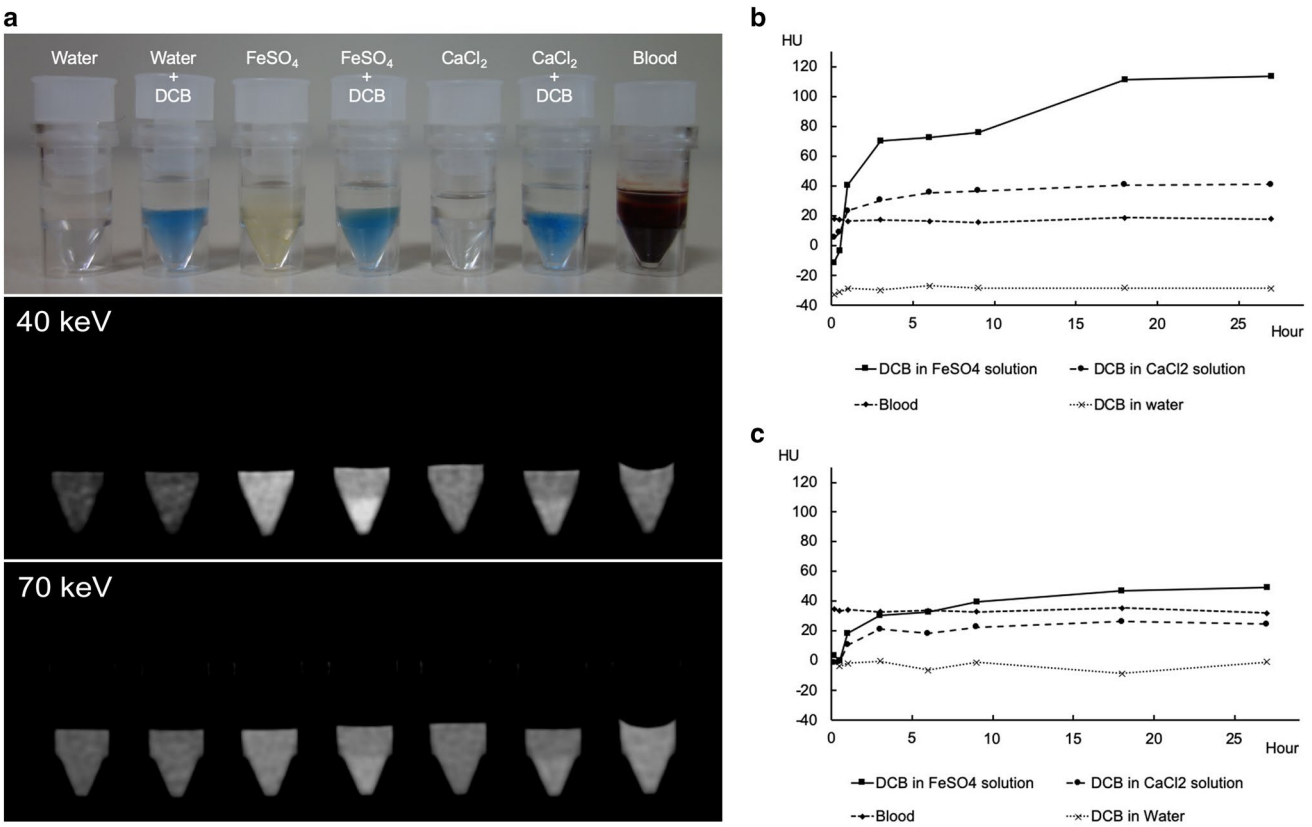

Fig. 1 The visibility of Fe^{2+}- or Ca^{2+}-loaded DCBs on DECT scan. Waters, $FeSO_4$ solutions and $CaCl_2$ solutions containing and not containing DCB, and blood are shown on the upper row; those images on 40- and 70-keV images from DECT at 27 h after mixing are shown on the middle and lower rows, respectively (**a**). The CT values of Fe^{2+}- or Ca^{2+}-loaded DCBs gradually increased on 40- (**b**) and 70-keV (**c**) images and achieved plateau values at 27 h. The CT value difference between Fe^{2+}-loaded DCB and blood on the 40-keV image is highest at 27 h. *HU* Hounsfield unit, *DCB* DC beads, *DECT* dual energy computed tomography

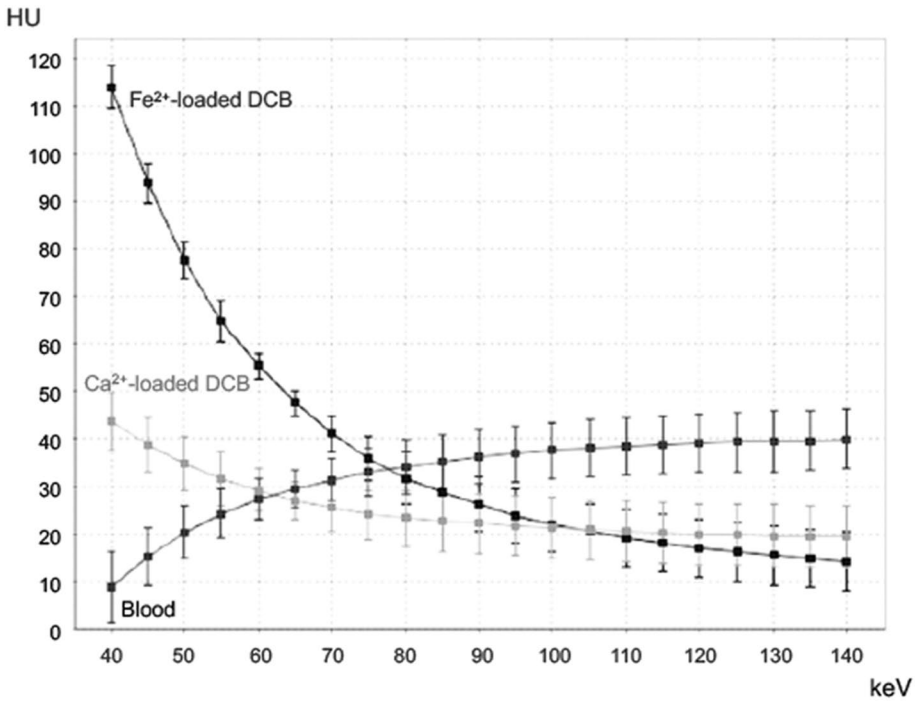

Fig. 2 The spectral HU curve at 27 h after mixing. The CT value of Fe^{2+}-loaded DCB increases exponentially and more steeply than that of Ca^{2+}-loaded DCB as photon energy decreases. The CT value of fresh venous blood decreases as photon energy decreases

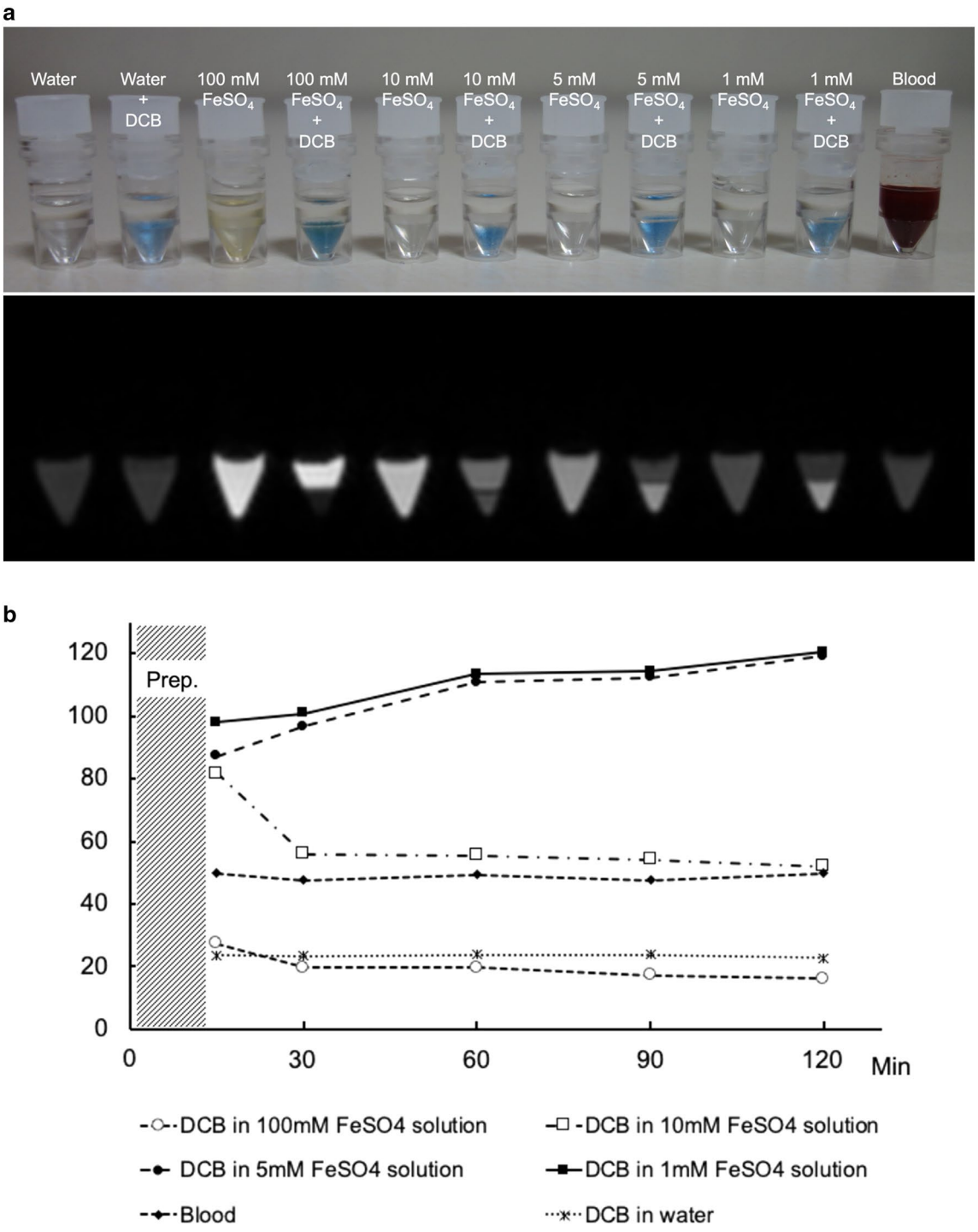

Fig. 3 The visibility of Fe^{2+}-loaded DCBs on T1-GRE MRI. Waters, 100, 10, 5, and 1 mM $FeSO_4$ solutions containing and not containing DCB, and blood are shown on the upper row; those images on T1-GRE at 120 min after mixing are shown on the lower row (**a**). The SNRs of Fe^{2+}-loaded DCBs in 1 and 5 mM $FeSO_4$ solutions gradually increase while the SNRs of Fe^{2+}-loaded DCBs in 100 and 10 mM $FeSO_4$ solutions decrease in processing time and they achieve plateau values at 120 min (**b**). *Prep* preparation time, *T1-GRE* T1-weighted gradient-echo, *SNRs* signal–noise ratios

constituents and non-poisoning, we thought that Fe^{2+} or Ca^{2+}-loaded DCB is safer than the other CT or MRI visible embolic agents. We evaluated the visibility of DCBs loaded with these mineral ions on low-keV monochromatic images from DECT and T1-GRE MRI, and demonstrated that the DCBs optimally loaded with Fe^{2+} ions are visible

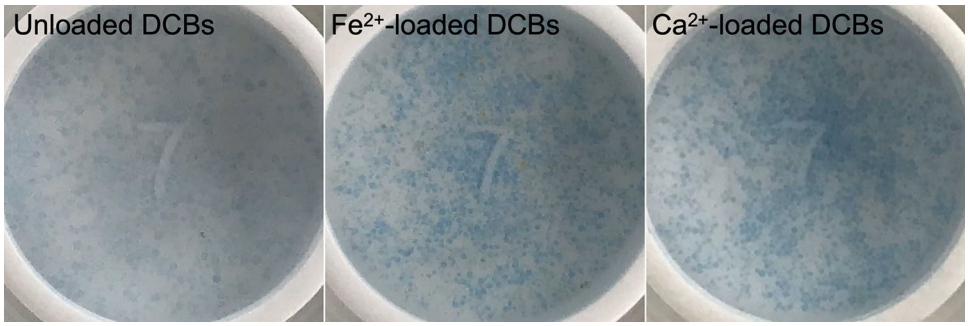

Fig. 4 Unloaded, Fe^{2+}-loaded, and Ca^{2+}-loaded DCB particles on microphotography. All kinds of particles do not aggregate each other in distilled water. Fe^{2+}-loaded and Ca^{2+}-loaded DCB particles maintained as the same size and shape as unloaded DCB particles

and discriminated from fresh venous blood on the 40-keV monochromatic image from DECT and T1-GRE in vitro study.

On the 40-keV monochromatic image from DECT, The CT value of Fe^{2+}-loaded DCB was higher than that of Ca^{2+}-loaded DCB. Fe^{2+} ion has a larger atomic number and binds more strongly with sulfonyl base of DCB than Ca^{2+} ion. Furthermore, Fe^{2+} ions covalently bound with DCB show a higher radiopacity due to higher density and atomic number as compared with Ca^{2+} ions [17]. Fe^{2+} ions eluted from Fe^{2+}-loaded DCB are considered safe in vivo, and the CT value differences between Fe^{2+}-loaded DCB at 27 h after mixing and fresh venous blood was 95.5 HU on a 40-keV monochromatic image, that was enough to be discriminated.

In this DECT study, our production method required 27 h since DCB was highly loaded with Fe^{2+} ions and the CT value achieved nearly equilibrium on the 40-keV monochromatic image. Although the loading time could be reduced when repeatedly stirring DCB in a denser $FeSO_4$ solution, we think that our loading method can constantly reproduce Fe^{2+}-loaded DCB visible on the 40-keV monochromatic image.

The CT values of Fe^{2+}- and Ca^{2+}-loaded DCBs are 49.1 and 24.4 HU on the 70-keV image from DECT. Considering the results, in vivo and ex vivo visualization of Fe^{2+}- and Ca^{2+}-loaded DCBs on X-ray fluoroscopy must be poor, and it is likely to be difficult to monitor the Fe^{2+}- and Ca^{2+}-loaded DCBs in vivo during TAE procedure; that is the weakest point of Fe^{2+}- and Ca^{2+}-loaded DCBs as compared with DC Bead LUMI® [5–7].

The SNRs of Fe^{2+}-loaded DCBs in 1 mM and 5 mM $FeSO_4$ solutions gradually increase in processing time and they achieve equilibrium at 120 min after mixing on T1-GRE. We think it is because of T1-shortening effect. On the other hand, the SNRs of Fe^{2+}-loaded DCB in 100 mM and 10 mM $FeSO_4$ solutions gradually decrease on T1-GRE; that is considered to be due to T2- and T2*-shortening effects of a large amount of Fe^{2+} ions bound with DCB.

The SNRs of DCBs loaded with Fe^{2+} ions in 100 mM $FeSO_4$ solution and in 1 mM $FeSO_4$ solution at 120 min after mixing was 33.7 lower and 70.8 higher than that of fresh venous blood, respectively. Although the SNR difference between Fe^{2+}-loaded DCB in 100 mM $FeSO_4$ solution and fresh venous blood was smaller than that between Fe^{2+}-loaded DCB in 1 mM $FeSO_4$ solution and fresh venous blood, the Fe^{2+}-loaded DCB loaded in 100 mM $FeSO_4$ solution may be utilized as a positive contrast embolization material on the 40-keV monochromatic image and as a negative contrast material on T1-GRE when being administrated in human arteries.

In our produced Fe^{2+}- or Ca^{2+}-loaded DCBs, these cations covalently bind to sulfonyl groups of DCB, and free anionic sulfonyl groups can be bound with positively charged anticancer drugs such as doxorubicin and irinotecan may be a few. We must investigate whether clinically effective amount of these drugs bind to earlier Fe^{2+}- or Ca^{2+}-loaded DCBs. DC Bead LUMI® is the spherical particles consist of polyvinylalcohol, which incorporates triiodobenzoyl and sulfonyl groups; the former makes the content of approximately 150 mg iodine/ml sedimented beads and leads to the bead visible in real time CT scan and the latter makes the cationic drugs bond to the bead and controls intratumoral release of the drugs [5–7]. DC Bead LUMI® may be superior to Fe^{2+}-loaded DCB for the drug delivery potential in DEB-TACE.

There are several limitations in this study. First, although we scanned Fe^{2+}- and Ca^{2+}-loaded DCBs in small containers using DECT with a small FOV or a 3 T-MR scanner and a head coil to avoid the artifacts from surrounding air, in vivo administrated DCBs must be scanned using DECT with a larger FOV and a larger MR receiver coil. Second, we only performed preliminary in vitro study concerning the bonding character of Fe^{2+} and Ca^{2+} ions to DCBs and demonstrated that Fe^{2+}-loaded DCB is desirably visible on 40-keV monochromatic images from DECT and T1-GRE. In vivo characteristics and visibility of Fe^{2+}-loaded DCBs are still unclear. We should perform in vivo animal studies (e.g., embolization of in vivo organs such as animal kidneys or implanted VX2 tumors) and investigate the visibility and utility of Fe^{2+}-loaded DCBs.

Conclusion

Optimally Fe^{2+}-loaded DCBs are opaque on 40-keV monochromatic images from DECT and T1-GRE MRI, and may make it easy to quantify the effect of embolization.

Compliance with ethical standards

Conflict of interest All authors declare that they have no conflict of interest.

References

1. Fako V, Wang XW. The status of transarterial chemoembolization treatment in the era of precision oncology. Hepat Oncol. 2017;4:55–63.
2. Malagari K, Iezzi R, Goldberg SN, Bilbao JI, Sami A, Akhan O, et al. The ten commandments of chemoembolization: expert discussion and report from Mediterranean Interventional Oncology (MIOLive) congress 2017. Eur Rev Med Pharmacol Sci. 2018;22:372–81.
3. Caine M, Carugo D, Zhang X, Hill M, Dreher MR, Lewis AL. Review of the development of methods for characterization of microspheres for use in embolotherapy: translating bench to Cathlab. Adv Healthc Mater. 2017;6:1601291.
4. Melchiorre F, Patella F, Pescatori L, Pesapane F, Fumarola E, Biondetti P, et al. DEB-TACE: a standard review. Future Oncol. 2018;14:2969–84.
5. Lewis AL, Willis SL, Dreher MR, Tang Y, Ashrafi K, Wood BJ, et al. Bench-to-clinic development of imageable drug-eluting embolization beads: finding the balance. Future Oncol. 2018;14:2741–60.
6. Hagan A, Phillips GJ, Macfarlane WM, Lloyd AW, Czuczman P, Lewis AL. Preparation and characterisation of vandetanib-eluting radiopaque beads for locoregional treatment of hepatic malignancies. Eur J Pharm Sci. 2017;101:22–30.
7. Iezzi R, Pompili M, Annicchiarico EB, Garcovich M, Siciliano M, Gasbarrini A, et al. 'Hug sign': a new radiological sign of intraprocedural success after combined treatment for hepatocellular carcinoma. Hepat Oncol. 2017;4:69–73.
8. Benzina A, Heijboer R, Koole LH. Engineering iodine-containing 3D-crosslinked methacrylic microspheres for transarterial embolization. Evaluation of fluoroscopic (X-ray) visibility in a hospital setting. Int J Nano Med Eng. 2017;2:171–6.
9. Sharma KV, Dreher MR, Tang Y, Pritchard W, Chiesa OA, Karanian J, et al. Development of "imageable" beads for transcatheter embolotherapy. J Vasc Interv Radiol. 2010;21:865–76.
10. Johnson CG, Tang Y, Beck A, Dreher MR, Woods DL, Negussie AH, et al. Preparation of radiopaque drug-eluting beads for transcatheter chemoembolization. J Vasc Interv Radiol. 2016;27(117–26):e3.
11. Zeng J, Li L, Zhang H, Li J, Liu L, Zhou G, et al. Radiopaque and uniform alginate microspheres loaded with tantalum nanoparticles for real-time imaging during transcatheter arterial embolization. Theranostics. 2018;8:4591–600.
12. Vollherbst DF, Gockner T, Do T, Holzer K, Mogler C, Flechsig P, et al. Computed tomography and histopathological findings after embolization with inherently radiopaque 40 µm-microspheres, standard 40 µm-microspheres and iodized oil in a porcine liver model. PLoS ONE. 2018;13:e0198911.
13. Cilliers R, Song Y, Kohlmeir EK, Larson AC, Omary RA, Meade TJ. Modification of embolic-PVA particles with MR contrast agents. Magn Reson Med. 2008;59:898–902.
14. Nijsen JF, Seppenwoolde JH, Havenith T, Bos C, Bakker CJ, van het Schip AD. Liver tumors: MR imaging of radioactive holmium microspheres-phantom and rabbit study. Radiology. 2004;231:491–9.
15. Lee KH, Liapi E, Vossen JA, Buijs M, Ventura VP, Georgiades C, et al. Distribution of iron oxide-containing embosphere particles after transcatheter arterial embolization in an animal model of liver cancer: evaluation with MR imaging and implication for therapy. J Vasc Interv Radiol. 2008;19:1490–6.
16. Hecq JD, Lewis AL, Vanbeckbergen D, Athanosopoulos A, Galanti L, Jamart J, et al. Doxorubicin-loaded drug-eluting beads (DC Bead®) for use in transarterial chemoembolization: a stability assessment. J Oncol Pharm Pract. 2013;19:65–74.
17. Bushberg JT. The AAPM/RSNA physics tutorial for residents. X-ray interactions. Radiographics. 1998;18:457–68.